

Phase estimation of Mach-Zehnder interferometer via Laguerre excitation squeezed state

Zekun Zhao¹, Huan Zhang², Yibing Huang^{1,*} and Liyun Hu^{1†}

¹Center for Quantum Science and Technology, Jiangxi Normal University, Nanchang 330022, China

²School of Physics, Sun Yat-sen University, Guangzhou 510275, China

Quantum metrology has an important role in the fields of quantum optics and quantum information processing. Here we introduce a kind of non-Gaussian state, Laguerre excitation squeezed state as input of traditional Mach-Zehnder interferometer to examine phase estimation in realistic case. We consider the effects of both internal and external losses on phase estimation by using quantum Fisher information and parity detection. It is shown that the external loss presents a bigger effect than the internal one. The phase sensitivity and the quantum Fisher information can be improved by increasing the photon number and even surpass the ideal phase sensitivity by two-mode squeezed vacuum in a certain region of phase shift for realistic case.

PACS: 03.67.-a, 05.30.-d, 42.50.Dv, 03.65.Wj

I. INTRODUCTION

Optical quantum metrology is one of the most important branches in the field of quantum science, which plays a key role for the advanced development of science and technology application. It is characteristics of using quantum systems or quantum mechanical properties, such as entanglement, squeezing or nonclassical property, to achieve high precision measurements of physical parameters, by minimizing the measurement uncertainty. It is shown that the precision of measurement can break through the standard quantum limit (SQL) due to the quantum effects. Based on this interesting point, the researchers focus their attention on the improvement of measurement precision by using quantum properties.

To realize this purpose above, the Mach-Zehnder interferometer (MZI) is widely used in various tasks of quantum measurement [1–4]. Generally, the measurement process can be divided into three parts, i.e., the preparation of input states, the interaction between the input state and the considered system, and the detection on the output state [5, 6]. Thus, it is natural to examine these three parts separately or collectively for enhancing the measurement precision. For instance, when injecting separately the coherent state and the squeezed state into two input ports of MZI [7], the phase precision can beat the SQL of $1/\sqrt{\bar{N}}$, with \bar{N} being the average photon-number of the input state. After that, many different quantum states have been proposed as the input states of MZI to achieve better performance. Among them, the NOON state [8], twin Fock state [9], and the two-mode squeezed vacuum state (TMSV) [10] *et al.* can achieve or even exceed the Heisenberg limit (HL) $1/\bar{N}$ [11–13], which have been verified by many experiments [14, 15]. However, on one hand, it is difficult to prepare a high average photon-number of quantum states of light [16]. On the other hand, the precision will be quickly

destroyed due to the inevitable interaction between the systems and the environments [16–21]. For example, for the TMSV, the experimentally available squeezing parameter is approximately 1.15 corresponding to a small average photon-number about $2 \sinh^2 r \approx 4$ [16]. In addition, the phase sensitivity is unstable relative to the phase shift. That is to say, the phase sensitivity will deteriorate rapidly when deviating from the optimal phase shift [22]. Thus, it is still a challenging task how to further improve the measurement precision and the ability against the decoherence.

Actually, the high nonclassical property including entanglement play an important role in various quantum information tasks, including quantum key distribution [23], quantum teleportation [24], and quantum metrology [7–10, 25–36]. Thus, preparing a kind of high nonclassical property state as inputs is an effective method to improve the measurement precision. For example, mixing photon-added/subtracted squeezed vacuum and coherent state as inputs, it is found that the phase sensitivity can be improved [25, 32–34]. Using photon-added/subtracted TMSV input the MZI can improve the precision of phase estimation [26, 27]. Recently, by employing multi-photon catalysis (MC) operating on the TMSV (MC-TMSV) as inputs of MZI [35], Zhang *et al.* studied the phase measurement including the case of photon losses. It is shown that the influences of photon losses before parity detection (external dissipation) on phase measurement accuracy is more serious than that after phase shifter (internal dissipation), but these effects can be suppressed by increasing the number of catalytic photons. In addition, the photon-number conversing operation is also used to improve phase estimation [36].

These above research works indicate that non-Gaussian operation is an effective way to improve the measurement precision. Inspired by this, we introduce a kind of non-Gaussian operation, i.e., Laguerre polynomial excitation operating on the TMSV as inputs of MZI, to improve the phase sensitivity. In fact, Laguerre polynomial excitation can achieve high nonclassicality and be theoretically realized [37, 38]. We shall investigate the phase sensitivity with parity detection and the quantum Fisher information (QFI) in both ideal and realistic

*huangyb@aliyun.com

†hlyun@jxnu.edu.cn

cases, by deriving an equivalent operator with the aid of the Weyl ordering invariance under similarity transformations. It is found that the phase sensitivity and the QFI can be improved whose effects become more obvious as the excited order.

This paper is organized as follows. In Sec. II, we first introduce the Laguerre polynomial excitation squeezed state. Then, we examine the QFI and the phase sensitivity with parity measurement in ideal case, when considering Laguerre polynomial excitation squeezed state as inputs. In Sec. III, we further consider the effects of photon losses on the phase sensitivity including external and internal dissipations. In Sec. IV, we investigate the influence of photon losses on the QFI. The main results are summarized in the last section.

II. PHASE ESTIMATION WHEN THE LAGUERRE POLYNOMIAL EXCITATION SQUEEZED STATE AS INPUTS OF MZI IN IDEAL CASE

A. Laguerre polynomial excitation squeezed state as Two-mode squeezed twin-Fock state

Actually, the Laguerre polynomial excitation squeezed state $|\text{Lagu}\rangle$ can be generated by applying two-mode squeezing operator on twin-Fock state $|n, n\rangle$, i.e.,

$$|\text{Lagu}\rangle = S(r) |n, n\rangle, \quad (1)$$

where $S(r) = \exp\{r(a^\dagger b^\dagger - ab)\}$ is the two-mode squeezing operator and $|n, n\rangle = |n\rangle_a \otimes |n\rangle_b$ is twin-Fock state. Using the coherent state representation of Fock state, i.e.,

$$|n\rangle_a = \frac{\partial^n}{\sqrt{n!} \partial \tau^n} \|\tau\rangle \Big|_{\tau=0}, \quad \|\tau\rangle = e^{\tau a^\dagger} |0\rangle_a, \quad (2)$$

and the transform relations

$$\begin{aligned} S(r) a S^\dagger(r) &= a \cosh r - b^\dagger \sinh r, \\ S(r) b S^\dagger(r) &= b \cosh r - a^\dagger \sinh r, \end{aligned} \quad (3)$$

Eq. (1) can be rewritten as the following form

$$|\text{Lagu}\rangle = (-\tanh r)^n L_n(ua^\dagger b^\dagger) S|00\rangle, \quad (4)$$

where we have used $u = 2/\sinh 2r$, $S|00\rangle = \text{sech}r \exp\{a^\dagger b^\dagger \tanh r\} |00\rangle$ and the formula $e^{A+B} = e^A e^B e^{-1/2[A,B]}$, which is valid for $[A, [A, B]] = [B, [A, B]] = 0$, as well as $e^{\lambda a} a^\dagger e^{-\lambda a} = a^\dagger + \lambda$, and

$$L_n(xy) = \frac{(-1)^n}{n!} \frac{\partial^{2n}}{\partial \tau^n \partial t^n} e^{-\tau t + \tau x + t y} \Big|_{\tau=t=0}, \quad (5)$$

with $L_n(xy)$ being Laguerre polynomials. From Eq. (4) it is clear that Laguerre polynomial excitation squeezed state is just the two-mode squeezed Fock state [39]. It is interesting that the twin-Fock states with 6 photons can

be achieved experimentally [14, 40]. Thus, the Laguerre polynomial excitation squeezed state can be successfully realized.

Using Eq. (1) and Eq. (3) it is ready to have the total average photon number, i.e.,

$$\begin{aligned} \bar{N} &= \langle \text{Lagu} | (a^\dagger a + b^\dagger b) | \text{Lagu} \rangle \\ &= 2n \cosh 2r + 2 \sinh^2 r. \end{aligned} \quad (6)$$

It is clear that the total average photon number of input state increases with r and n .

B. Laguerre polynomial excitation squeezed state as input of MZI and parity detection

In order to establish the basis of studying the phase estimation via Laguerre polynomial excitation squeezed state in the non-ideal case, here we consider the Laguerre polynomial excitation squeezed state as input of MZI for discussing the effect of this non-Gaussian state on the precision of measurement in the ideal case. As shown in Fig. 1, the traditional MZI consist of two symmetrical beam splitters (BSs) (denoted as BS1 and BS2), two input ports (mode a and b) and two completely reflecting mirrors as well as two-phase shifters. Here we should note that the two BSs are conjugated to each other.

For this ideal MZI in Fig. 1, according to Ref. [41], the effect is equivalent to a BS operator, i.e.,

$$U_{MZI} = e^{i\pi J_1/2} e^{-i\varphi J_3} e^{-i\pi J_1/2} = e^{-i\varphi J_2}, \quad (7)$$

where J_1, J_2, J_3 are Bosonic operators, defined as

$$\begin{aligned} J_1 &= \frac{1}{2} (a^\dagger b + ab^\dagger), \\ J_2 &= \frac{1}{2i} (a^\dagger b - ab^\dagger), \\ J_3 &= \frac{1}{2} (a^\dagger a - b^\dagger b). \end{aligned} \quad (8)$$

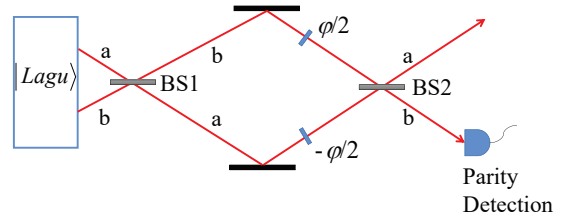


FIG. 1: Schematic diagram of a balanced MZI for the parity detection of the phase shift when the Laguerre excitation squeezed state is injected into the first beam splitter.

1. The quantum Fisher information

Here we examine the QFI when inputting $|\text{Lagu}\rangle$ into the MZI in ideal case. For the model shown in Fig. 1,

the QFI F_Q describes the amount of information containing phase parameters carried by light after it passes through the phase shifter. The quantum Cramér-Rao bound (QCRB) gives the highest theoretical measurement accuracy of phase shifts, which is expressed by the QFI [6], i.e.,

$$\Delta\varphi_{QCRB} = \frac{1}{\sqrt{F_Q}}. \quad (9)$$

For the pure state as the input state $|in\rangle$ of MZI, the QFI F_Q can be calculated by

$$F_Q = 4 \left[\langle \psi'(\varphi) | \psi'(\varphi) \rangle - |\langle \psi'(\varphi) | \psi(\varphi) \rangle|^2 \right], \quad (10)$$

where $|\psi(\varphi)\rangle = e^{-i\varphi J_3} e^{-i\pi J_1/2} |in\rangle$ is the quantum state after the evolution of the first BS and phase shifter, $|\psi'(\varphi)\rangle = \partial|\psi(\varphi)\rangle/\partial\varphi$. Therefore, it can be known that in the case of $|Lagu\rangle$ as the input state of MZI, the expression of the QFI can be derived as

$$F_Q = [2 + 3 \sinh^2(2r)] n(n+1) + \sinh^2(2r). \quad (11)$$

2. The phase sensitivity with parity detection

Through this paper, we shall take parity detection as measurement method. Here, we consider the parity detection at output mode b . Actually, the photon-number parity operator is given by

$$\Pi_b = (-1)^{b^\dagger b} = e^{i\pi b^\dagger b}, \quad (12)$$

whose normal ordering form is

$$\Pi_b = : \exp\{-2b^\dagger b\} : , \quad (13)$$

where $: \cdot :$ is the symbol of the normal ordering. Thus using the formula converting operator \hat{O} from normal ordering to its Weyl ordering form, i.e.,

$$\hat{O} = 2 : \int \frac{d^2\alpha}{\pi} \langle -\alpha | \hat{O} | \alpha \rangle e^{2(\alpha^* b - b^\dagger \alpha + b^\dagger b)} : , \quad (14)$$

where $|\alpha\rangle$ is the coherent state, the Weyl ordering form of parity operator Π_b can be derived as

$$\Pi_b = \frac{\pi}{2} : \delta(b) \delta(b^\dagger) : , \quad (15)$$

where $: \dots :$ is the symbol of the Weyl ordering and $\delta(\cdot)$ is the delta function [42, 43].

Noticing the Weyl ordering invariance under similarity transformations [44, 45], i.e.,

$$U_{MZI}^\dagger : \dots : U_{MZI} = : U_{MZI}^\dagger \dots U_{MZI} : , \quad (16)$$

and the transformation relations

$$\begin{aligned} e^{i\varphi J_2} a e^{-i\varphi J_2} &= a \cos \frac{\varphi}{2} - b \sin \frac{\varphi}{2}, \\ e^{i\varphi J_2} b e^{-i\varphi J_2} &= b \cos \frac{\varphi}{2} + a \sin \frac{\varphi}{2}, \end{aligned} \quad (17)$$

then the parity operator under the unitary transformation is changed to be

$$\begin{aligned} \Pi_b &\rightarrow \Pi_{MZI} \equiv U_{MZI}^\dagger \Pi_b U_{MZI} \\ &= \frac{\pi}{2} : \delta \left(b \cos \frac{\varphi}{2} + a \sin \frac{\varphi}{2} \right) \\ &\quad \times \delta \left(b^\dagger \cos \frac{\varphi}{2} + a^\dagger \sin \frac{\varphi}{2} \right) : , \end{aligned} \quad (18)$$

which is just the Weyl ordering form of the parity operator Π_b under the unitary transformation U_{MZI} .

For a Weyl ordering operator, say $: f(a, a^\dagger, b, b^\dagger) :$, its classical correspondence can be obtained by replacing $a, a^\dagger, b, b^\dagger$ with complex parameters $\alpha, \alpha^*, \beta, \beta^*$, respectively, i.e., $: f(a, a^\dagger, b, b^\dagger) : \rightarrow f(\alpha, \alpha^*, \beta, \beta^*)$. Further using the relation between classical correspondence and Wigner operator [45], i.e.,

$$\begin{aligned} &: f(a, a^\dagger, b, b^\dagger) : \\ &= 4 \int d^2\alpha d^2\beta f(\alpha, \alpha^*, \beta, \beta^*) \Delta_a(\alpha) \Delta_b(\beta), \end{aligned} \quad (19)$$

where $\Delta_{a/b}(\alpha/\beta)$ is the Wigner operators whose normal ordering form is given by [46, 47]

$$\begin{aligned} \Delta_a(\alpha) &= \frac{1}{\pi} : \exp[-2(a - \alpha)(a^\dagger - \alpha^*)] : , \\ \Delta_b(\beta) &= \frac{1}{\pi} : \exp[-2(b - \beta)(b^\dagger - \beta^*)] : , \end{aligned} \quad (20)$$

and using the integration within an ordered product (IWOP) technique [47, 48] as well as the following integral formula [49]

$$\int \frac{d^2z}{\pi} e^{\zeta|z|^2 + \xi z + \eta z^* + f z^2 + g z^{*2}} = \frac{e^{-\frac{\zeta\xi\eta + \xi^2g + \eta^2f}{\zeta^2 - 4fg}}}{\sqrt{\zeta^2 - 4fg}}, \quad (21)$$

the normal ordering of Π_{MZI} can be obtained, i.e.,

$$\begin{aligned} \Pi_{MZI} &= : \exp[(-\sin\varphi - 1)a^\dagger a + (\sin\varphi - 1)b^\dagger b] \\ &\quad \times \exp[-(b^\dagger a + a^\dagger b) \cos\varphi] : . \end{aligned} \quad (22)$$

According to Ref. [10], we has made a shift transformation $\varphi \rightarrow \varphi + \pi/2$ in Eq. (22). When the state $|Lagu\rangle$ as input of MZI, the expectation value of parity operator in the output state can be expressed as $\langle \Pi_0 \rangle = \langle Lagu | U_{MZI}^\dagger \Pi_b U_{MZI} | Lagu \rangle = \langle Lagu | \Pi_{MZI} | Lagu \rangle$, where $\Pi_{MZI} = U_{MZI}^\dagger \Pi_b U_{MZI}$

whose normal ordering form is given in Eq. (22). Inserting the completeness relation of coherent state and using Eq. (21), $\langle \Pi_0 \rangle$ can be calculated as

$$\begin{aligned} \langle \Pi_0 \rangle &= A_0 \hat{D}_n \{ \exp [(x^2 + t^2 - y^2 - \tau^2) A_1] \\ &\quad \times \exp [(xy + t\tau) A_2] \\ &\quad \times \exp [(y\tau - xt) A_3] \\ &\quad \times \exp [(x\tau + yt) A_4] \}, \end{aligned} \quad (23)$$

where $\hat{D}_n \{ \cdot \} = \frac{\partial^{4n}}{(n!)^2 \partial x^n \partial y^n \partial t^n \partial \tau^n} \{ \cdot \} |_{x=y=t=\tau=0}$, and

$$\begin{aligned} A_0 &= \frac{\text{sech}^2 r}{\sqrt{\omega_0}}, \\ A_1 &= \frac{\sin(2\varphi) \tanh r}{2\omega_0 \cosh^2 r}, \\ A_2 &= \frac{(\cos(2\varphi) - 1)(\tanh r + \tanh^3 r)}{\omega_0}, \\ A_3 &= \frac{\sin \varphi \cosh(2r) \text{sech}^4 r}{\omega_0}, \\ A_4 &= \frac{-\cos \varphi \text{sech}^4 r}{\omega_0}, \end{aligned} \quad (24)$$

as well as $\omega_0 = 1 - 2 \tanh^2 r \cos(2\varphi) + \tanh^4 r$. Thus, using Eq. (23) we can get the phase sensitivity $\Delta\varphi_0$ via error propagation formula, i.e.,

$$\Delta\varphi_0 = \frac{\Delta\Pi_0}{|\partial \langle \Pi_0 \rangle / \partial \varphi|}, \quad (25)$$

where $\Delta\Pi_0 = \sqrt{1 - \langle \Pi_0 \rangle^2}$. From the value of $\Delta\varphi_0$, in principle, we can know the phase measurement accuracy of Laguerre polynomial excitation squeezed state as input of MZI.

In particular, when $n = 0$ corresponding to the TMSV as input of MZI, the phase sensitivity with parity detection is given by

$$\Delta\varphi_{TMSV} = \frac{\omega_0 \cosh^2 r}{2 \tanh r \cos \varphi}, \quad (26)$$

as expected [10].

III. EFFECTS OF PHOTON LOSSES ON PHASE SENSITIVITY

In the process of quantum precision measurement, photon losses is inevitable. It is of great practical significance to study the influence of photon losses on phase sensitivity. In this section, we consider the phase sensitivity with Laguerre polynomial excitation squeezed state as input of MZI in photon losses case. Here, we only examine that the photon losses occurs either before parity detection in MZI (outside the interferometer) or between the phase shift and the second BS (inside the interferometer), shown in Fig. 2.

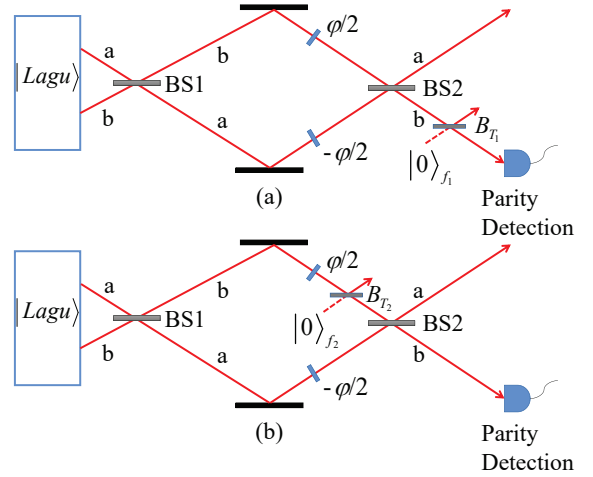


FIG. 2: Schematic diagram of the parity detection in the presence of photon losses. (a) External dissipation: photon losses occur between the parity detection and the BS2. (b) Internal dissipation: photon losses occur between the phase shifter and the BS2.

A. Effects of photon losses before parity detection (external dissipation)

First, we focus on the case with photon losses before parity detection as shown in Fig. 2 (a) and investigate the effects of photon losses on the phase sensitivity. It will be convenient to redefine an equivalent parity operator including photon losses, which is different from the ideal case where parity operator is $\Pi_b = (-1)^{b^\dagger b}$. For this purpose, we use an optical BS B_{T_1} to simulate the photon losses at the probe end, shown in Fig. 2(a). The corresponding transform relation by B_{T_1} is given by

$$B_{T_1}^\dagger \begin{pmatrix} b \\ f_1 \end{pmatrix} B_{T_1} = \begin{pmatrix} \sqrt{T_1} & \sqrt{1-T_1} \\ -\sqrt{1-T_1} & \sqrt{T_1} \end{pmatrix} \begin{pmatrix} b \\ f_1 \end{pmatrix}, \quad (27)$$

where f_1 (f_1^\dagger) are photon annihilation (creation) operators corresponding to the dissipative mode f_1 of B_{T_1} and T_1 is the transmissivity of B_{T_1} . T_1 is related to external dissipation. The larger T_1 is, the smaller external photon losses is.

Using Eqs. (15) and (27), and the Weyl ordering invariance under similarity transformations, the equivalent parity operator including photon losses Π_b^{loss} can be calculated as

$$\begin{aligned} \Pi_b^{loss} &= \frac{\pi}{2} {}_{f_1} \langle 0 | \vdots B_{T_1}^\dagger \delta(b) \delta(b^\dagger) B_{T_1} \vdots | 0 \rangle_{f_1} \\ &= \frac{\pi}{2} {}_{f_1} \langle 0 | \vdots \delta(\sqrt{T_1} b + \sqrt{1-T_1} f_1) \\ &\quad \times \delta(\sqrt{T_1} b^\dagger + \sqrt{1-T_1} f_1^\dagger) \vdots | 0 \rangle_{f_1}, \end{aligned} \quad (28)$$

where $|0\rangle_{f_1}$ is vacuum noise inputting BS B_{T_1} . In a similar way to deriving Eq. (22), using Eqs. (19)-(21), the

normal ordering form of Π_b^{loss} is derived as

$$\Pi_b^{loss} =: \exp(-2T_1 b^\dagger b) : . \quad (29)$$

It is clear that for the case of $T_1 = 1$ corresponding to the photon lossless, Π_b^{loss} just reduces to $\Pi_b =: \exp(-2b^\dagger b) : ,$ as expected. Thus, the expectation value of parity detection in the case of photon loss can be transformed to be $\langle \Pi_b^{loss} \rangle = \langle \text{out} | \Pi_b^{loss} | \text{out} \rangle,$ where $|\text{out}\rangle$ is the output state after the second BS of MZI and before the photon loss.

In our scheme, using the completeness relation of coherent states, and combining the unitary transformations $U_{MZI} a^\dagger U_{MZI}^\dagger = a^\dagger \cos \frac{\varphi}{2} + b^\dagger \sin \frac{\varphi}{2},$ $U_{MZI} b^\dagger U_{MZI}^\dagger = b^\dagger \cos \frac{\varphi}{2} - a^\dagger \sin \frac{\varphi}{2}$ as well as the relation $U_{MZI} |0, 0\rangle = |0, 0\rangle,$ the output state can be shown as

$$\begin{aligned} |\text{out}\rangle &= \frac{\text{sech} r}{n!} \frac{\partial^{2n}}{\partial x^n \partial y^n} \int \frac{d^2 \alpha d^2 \beta}{\pi^2} \\ &\times \exp[-|\alpha|^2 - |\beta|^2 + \alpha^* \beta^* \tanh r \\ &- xy \tanh r + \alpha^* x \text{sech} r + \beta^* y \text{sech} r] \\ &\times \exp[(\alpha \cos \frac{\varphi}{2} - \beta \sin \frac{\varphi}{2}) a^\dagger \\ &+ (\alpha \sin \frac{\varphi}{2} + \beta \cos \frac{\varphi}{2}) b^\dagger] |00\rangle_{|x=y=0}. \quad (30) \end{aligned}$$

Thus, by further inserting the completeness relation of coherent states and using Eq. (21), the parity measurement in realistic case is calculated as

$$\langle \Pi_b^{loss} \rangle = C_1 \hat{D}_n \exp[C_2 + C_3 + C_4 + C_5], \quad (31)$$

where

$$\begin{aligned} C_1 &= \frac{\text{sech}^2 r}{\sqrt{\omega_1}}, \\ C_2 &= \frac{\mu_1 \varkappa_1}{\omega_1} [1 - (\epsilon_1^2 + \epsilon_2 \epsilon_3) \tanh^2 r], \\ C_3 &= \frac{\mu_1^2 \epsilon_1 \epsilon_2}{\omega_1} \tanh r, \\ C_4 &= \frac{\varkappa_1^2 \epsilon_1 \epsilon_3}{\omega_1} \tanh^3 r, \\ C_5 &= (\epsilon_1 x + \epsilon_3 y) \tau \text{sech}^2 r \\ &+ \epsilon_1 \epsilon_3 (\tau \text{sech} r)^2 \tanh r \\ &- (t\tau + xy) \tanh r, \quad (32) \end{aligned}$$

and

$$\begin{aligned} \omega_1 &= ((\epsilon_1^2 + \epsilon_2 \epsilon_3) \tanh^2 r - 1)^2 \\ &- 4\epsilon_1^2 \epsilon_2 \epsilon_3 \tanh^4 r, \\ \mu_1 &= (\epsilon_1 x + \epsilon_3 y) \text{sech} r \tanh r \\ &+ (2\epsilon_1 \epsilon_3 \tau \tanh^2 r + t) \text{sech} r, \\ \varkappa_1 &= (\epsilon_1^2 + \epsilon_2 \epsilon_3) \tau \text{sech} r \tanh r \\ &+ (\epsilon_2 x + \epsilon_1 y) \text{sech} r, \\ \epsilon_1 &= -T_1 \cos \varphi, \\ \epsilon_2 &= 1 - T_1 (1 + \sin \varphi), \\ \epsilon_3 &= 1 - T_1 (1 - \sin \varphi), \quad (33) \end{aligned}$$

where $\varphi \rightarrow \varphi + \pi/2$ is used again. In particular, when $T_1 = 1,$ i.e., the ideal case, Eq. (31) can be simplified to be Eq. (23). Furthermore, when $n = 0,$ Eq. (31) becomes $\langle \Pi_b^{loss} \rangle = \frac{\text{sech}^2 r}{\sqrt{\omega_0}},$ as expected. Using the expectation value $\langle \Pi_b^{loss} \rangle$ of parity operator under external photon losses in Eq. (31), we can further obtain the phase sensitivity $\Delta\varphi$ by using

$$\Delta\varphi = \frac{\Delta \Pi_b^{loss}}{|\partial \langle \Pi_b^{loss} \rangle / \partial \varphi|}, \quad (34)$$

which is similar to deriving Eq. (23).

According to Eq. (34), we can further investigate the phase sensitivity when the Laguerre polynomial excitation squeezed state as input of MZI. As shown in Fig. 3, for both ideal and realistic cases, the phase sensitivity $\Delta\varphi$ is plotted as the function of the squeezing parameter r and the transmissivity T_1 of B_{T_1} for some given parameters. From Fig. 3, it is clear that the phase sensitivity $\Delta\varphi$ in the case of external dissipation is worse than that in the ideal case ($T_1 = 1$). However, $\Delta\varphi$ can be still improved with the increase of the excited photon number n for any r . In addition, it is found from Fig. 3(b) that $\Delta\varphi$ can be improved with the increase of T_1 .

Fig. 4 presents the relation between the phase sensitivity $\Delta\varphi$ and the phase shift φ for different excited photon number n and T_1 as well as given parameter $r = 0.7$. From Fig. 4(a), it is shown that (i) in the ideal case ($T_1 = 1$), the optimal phase sensitivity is at the point with $\varphi = 0,$ and it becomes better as n increases. Compared with the TMSV as inputs, however, the improved region of $\Delta\varphi$ becomes smaller with the increase of n . (ii) For the realistic case (say $T_1 = 0.95$), the optimal point of the phase sensitivity will deviate from $\varphi = 0,$ and the $\Delta\varphi$ value corresponding to optimal point decreases with the increase of n . It is interesting to notice that, even in the realistic case, the phase sensitivity still surpass that by the TMSV in the ideal case, but the improved region of φ becomes smaller with the increase of n which is similar to the ideal case.

On the other hand, the energy is an important index to measure the phase sensitivity, here we further consider the phase estimation when fixing the total initial energy. Fig. 4(b) shows the phase sensitivity $\Delta\varphi$ as the

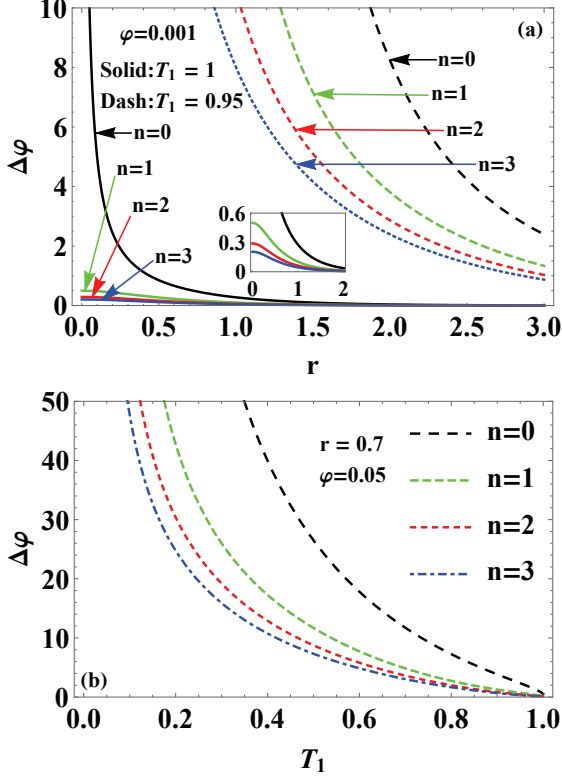


FIG. 3: For the photon number $n = 0, 1, 2, 3$, (a) the phase sensitivity $\Delta\varphi$ as a function of the squeezing parameters r , for the phase shift $\varphi = 0.001$, the transmissivity of B_{T_1} $T_1 = 1$ and $T_1 = 0.95$, (b) for $r = 0.7$ and $\varphi = 0.05$, $\Delta\varphi$ as a function of T_1 .

function of φ for different n and T_1 as well as given total average photon number $\bar{N} = 8$. It is found that (i) in the ideal case ($T_1 = 1$), the optimal phase sensitivity is at the point with $\varphi = 0$, but it becomes worse as n increases, which is the opposite to the above situation. However, it is interesting that the improved region of $\Delta\varphi$ becomes bigger with the increase of n , i.e., the phase sensitivity is more stable with respect to the phase shift. This implies that, when fixing the total initial energy, although the optimal phase sensitivity becomes worse, the improved region will become broader and more stable. (ii) In the realistic case (say $T_1 = 0.95$), it is clearly seen that external dissipation causes the optimal phase to deviate from $\varphi = 0$ and the optimal value of $\Delta\varphi$ decreases with the increase of n , i.e., the phase sensitivity becomes higher as n increases which is similar to the case in Fig. 4(a). In addition, the improved region becomes bigger as n increases, which is different from the case in Fig. 4(a). In a word, the phase sensitivity in the realistic case increases with the excited photon number, whether the initial energy is fixed or not.

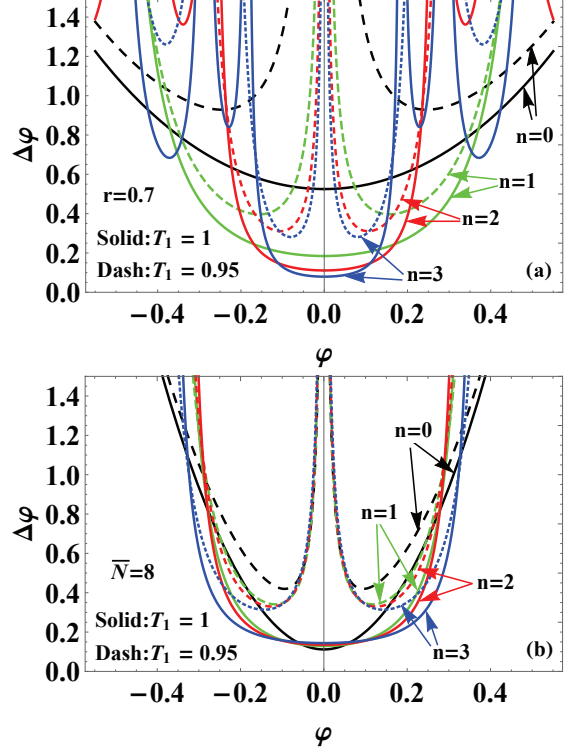


FIG. 4: The phase sensitivity $\Delta\varphi$ as a function of the phase shift φ , for the photon number $n = 0, 1, 2, 3$, the transmissivity of B_{T_1} $T_1 = 1$ and $T_1 = 0.95$ (a) Squeezing parameter $r = 0.7$, (b) the total average photon number $\bar{N} = 8$.

B. Effects of photon losses between phase shifter and BS2 (internal dissipation)

In this subsection, we examine the effects of photon losses between phase shifter and BS2 on the phase sensitivity. We name the photon losses between them as internal dissipation, as shown in Fig. 2(b). In a similar way, we adopt an optical BS B_{T_2} with a factor T_2 to simulate the internal photon-losses process, whose transform relation is

$$B_{T_2}^\dagger \begin{pmatrix} b \\ f_2 \end{pmatrix} B_{T_2} = \begin{pmatrix} \sqrt{T_2} & \sqrt{1-T_2} \\ -\sqrt{1-T_2} & \sqrt{T_2} \end{pmatrix} \begin{pmatrix} b \\ f_2 \end{pmatrix}, \quad (35)$$

where f_2 (f_2^\dagger) are photon annihilation (creation) operators corresponding to the dissipative mode f_2 of B_{T_2} and T_2 is the transmissivity of B_{T_2} . In this case, the average value of parity detection can be calculated as $\langle \tilde{\Pi}_b^{loss} \rangle = \langle \text{in} | \tilde{\Pi}_b^{loss} | \text{in} \rangle$, where $|\text{in}\rangle$ is the input state of MZI, and $\tilde{\Pi}_b^{loss}$ is the equivalent operator of the entire lossy interferometer, including parity detection, given by

$$\tilde{\Pi}_b^{loss} = f_2 \langle 0 | B_1^\dagger U^\dagger(\varphi) B_{T_2}^\dagger B_2^\dagger e^{i\pi b^\dagger b} B_2 B_{T_2} U(\varphi) B_1 | 0 \rangle_{f_2}, \quad (36)$$

where $B_1(-\pi/2) = e^{-i\frac{\pi}{2}J_1}$ and $B_2(\pi/2) = e^{i\frac{\pi}{2}J_1}$ are BS1 and BS2 operators, respectively, and satisfy the fol-

lowing transform relation:

$$\begin{aligned} B_1^\dagger \begin{pmatrix} a \\ b \end{pmatrix} B_1 &= \frac{\sqrt{2}}{2} \begin{pmatrix} 1 & -i \\ -i & 1 \end{pmatrix} \begin{pmatrix} a \\ b \end{pmatrix}, \\ B_2^\dagger \begin{pmatrix} a \\ b \end{pmatrix} B_2 &= \frac{\sqrt{2}}{2} \begin{pmatrix} 1 & i \\ i & 1 \end{pmatrix} \begin{pmatrix} a \\ b \end{pmatrix}, \end{aligned} \quad (37)$$

and $U(\varphi) = e^{-i\varphi J_3}$ is the phase shifter.

In a similar way to deriving Eq. (28), by using Eqs. (35)-(37) and (15), one can obtain the normal ordering of $\tilde{\Pi}_b^{loss}$, i.e.,

$$\tilde{\Pi}_b^{loss} =: e^{X_1 a^\dagger a - X_2 b^\dagger a - X_2^* a^\dagger b + X_3 b^\dagger b}, \quad (38)$$

where

$$\begin{aligned} X_1 &= -\frac{2\sqrt{T_2} \sin \varphi + 1 + T_2}{2}, \\ X_2 &= \frac{(T_2 + 1)^2 - 4T_2 \sin^2 \varphi}{2(iT_2 - i + 2\sqrt{T_2} \cos \varphi)}, \\ X_3 &= \frac{2\sqrt{T_2} \sin \varphi - 1 - T_2}{2}, \end{aligned} \quad (39)$$

where $\varphi \rightarrow \varphi + \pi/2$. In particular, when $T_2 = 1$ corresponding to the ideal case, we have $X_1 \rightarrow -\sin \varphi - 1$, $X_2 = \cos \varphi$, $X_3 = \sin \varphi - 1$. Then $\tilde{\Pi}_b^{loss} \rightarrow: e^{(-\sin \varphi - 1)a^\dagger a - \cos \varphi(b^\dagger a + a^\dagger b) + (\sin \varphi - 1)b^\dagger b}$, as expected (reduces to Eq. (22)).

In our scheme, the input state is given by Eq. (4). Thus, by using Eqs. (4), (21) and (38), and inserting completeness relation of coherent states, we can get the expectation value of $\tilde{\Pi}_b^{loss}$ under the input state, which is given by

$$\langle \tilde{\Pi}_b^{loss} \rangle = D_1 \hat{D}_n \{ \exp [D_2 + D_3 + D_4 + D_5] \}, \quad (40)$$

where

$$\begin{aligned} D_1 &= \frac{\text{sech}^2 r}{\sqrt{\omega_2}}, \\ D_2 &= \frac{\mu_2 \varkappa_2 (1 - E \tanh^2 r)}{\omega_2}, \\ D_3 &= \frac{-\mu_2^2 X_2 (X_3 + 1)}{\omega_2} \tanh r, \\ D_4 &= \frac{\varkappa_2^2 (-X_1 X_2^* - X_2^*)}{\omega_2} \tanh^3 r, \\ D_5 &= (-X_2^* y + X_1 x + x) t \text{sech}^2 r \\ &\quad + (-X_1 X_2^* - X_2^*) t^2 \text{sech}^2 r \tanh r \\ &\quad - xy \tanh r - t\tau \tanh r, \end{aligned} \quad (41)$$

and

$$\begin{aligned} \omega_2 &= (1 - E \tanh^2 r)^2 \\ &\quad - 4 |X_2|^2 (X_1 + 1) (X_3 + 1) \tanh^4 r, \\ \mu_2 &= (-X_2^* y + X_1 x + x) \text{sech} r \tanh r \\ &\quad - 2 (X_1 + 1) X_2^* t \tanh^2 r \text{sech} r + \tau \text{sech} r, \\ \varkappa_2 &= E t \text{sech} r \tanh r \\ &\quad + (X_3 + 1) y \text{sech} r - X_2 x \text{sech} r, \\ E &= |X_2|^2 + X_1 X_3 + X_3 + X_1 + 1. \end{aligned} \quad (42)$$

For the ideal case of $T_2 = 1$, Eq. (40) reduces to Eq. (23), as expected. In addition, when $n = 0$, Eq. (40) becomes $\langle \tilde{\Pi}_b^{loss} \rangle = \frac{\text{sech}^2 r}{\sqrt{\omega_2}}$. Eq. (40) is just the parity signal in the presence of internal dissipation, and it is ready to obtain the phase sensitivity combining Eqs. (34) and (40).

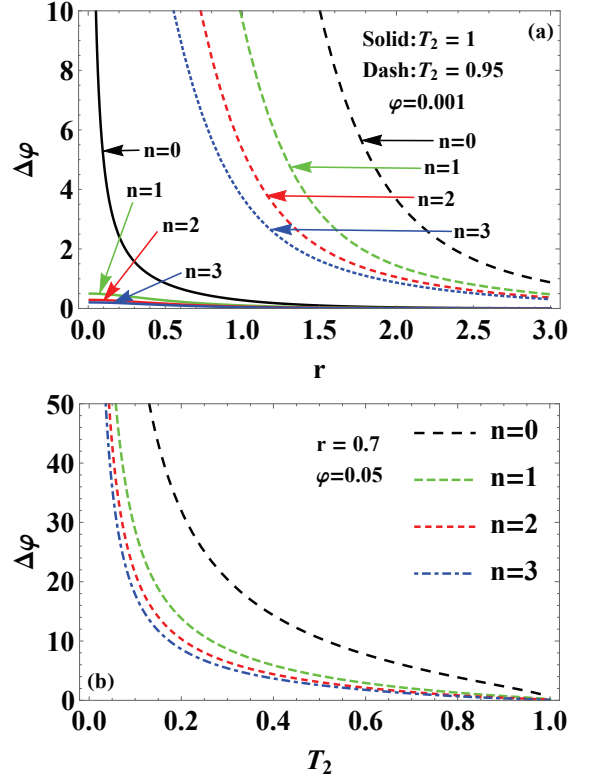


FIG. 5: For the photon number $n = 0, 1, 2, 3$, (a) the phase sensitivity $\Delta\varphi$ as a function of the squeezing parameters r , for the phase shift $\varphi = 0.001$, the transmissivity of B_{T_2} $T_2 = 1$ and $T_2 = 0.95$, (b) for $r = 0.7$ and $\varphi = 0.05$, $\Delta\varphi$ as a function of T_2 .

Similar to Figs. 3 and 4, Figs. 5 and 6 present $\Delta\varphi$ as a function of squeezing parameter, dissipative factor and phase shift for other given values. Some similar results can be obtained. Briefly, the phase sensitivity $\Delta\varphi$ can be enhanced by increasing excited photon number, and even surpass the ideal phase sensitivity by the TMSV in a certain region of φ .

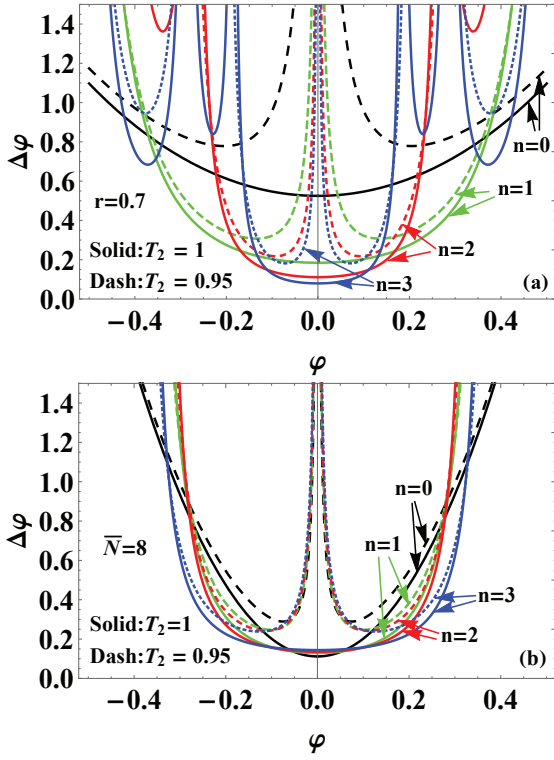


FIG. 6: The phase sensitivity $\Delta\varphi$ as a function of the phase shift φ , for the photon number $n = 0, 1, 2, 3$, the transmissivity of B_{T_2} $T_2 = 1$ and $T_2 = 0.95$, (a) for the squeezing parameter $r = 0.7$, (b) for the total average photon number $\bar{N} = 8$.

In addition, comparing Figs. 3 and 4 with Figs. 5 and 6, it is ready to see the difference between internal dissipation and external one on the phase sensitivity. It is found that the external dissipation has a greater impact on the phase measurement accuracy than the internal dissipation. To clearly see this point, at fixed $\varphi = 0.05$, $r = 0.7$, we give the phase sensitivity $\Delta\varphi$ as a function of T_1 (T_2) for several different $n = 0, 1, 2, 3$ as shown in Fig. 7. This result implies that, to get a better precision of phase measurement, special attention should be paid to the control of external photon losses.

In order to further clearly see the difference between internal and external dissipations, we plot the phase sensitivity $\Delta\varphi$ as a function of the squeezing parameter r for different excited photon number $n = 0, 1, 2, 3$ (optimized over the parameter φ) in Fig. 8. Here the SQL and the HL are also plotted for comparison. From Fig. 8, it is shown that (i) $\Delta\varphi$ can break the SQL and the HL for $n = 0$ [see Fig. 8(a)]. (ii) $\Delta\varphi$ can break through the SQL in a certain range of r . In particular, $\Delta\varphi$ with the internal dissipation can break through the SQL in a larger squeezing region than that with the external dissipation.

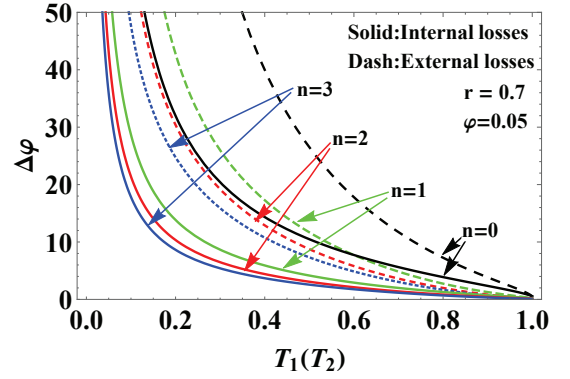


FIG. 7: Comparing the influence of two dissipation ways on the phase sensitivity $\Delta\varphi$ for the photon number $n = 0, 1, 2, 3$.

IV. EFFECTS OF PHOTON LOSSES ON THE QFI

The QFI theoretically gives the optimal accuracy of phase estimation independent of special measures, but this optimal accuracy is also affected by the photon losses in the realistic environment. In this section, we mainly consider the influences of photon losses along the path of photon interferometer on the QFI. As shown in Fig. 9, for simplicity, we assume that photon losses exist in the optical path of mode b , and the sources of photon losses is mainly located before and after the phase shift, which are respectively simulated by two optical BSs of B_{η_1} and B_{η_2} , where $\eta_1 = \eta_2 = \eta$ are transmissivities of B_{η_1} and B_{η_2} , related to the dissipation factor of photon losses.

According to the research on the bounds for error estimation in noisy systems of Escher *et al.* [50], in this case, the QFI F_Q can be calculated by the following equation:

$$F_Q \leq C_Q = 4 \left[\langle \psi | \hat{H}_1 | \psi \rangle - \langle \psi | \hat{H}_2 | \psi \rangle \right]^2, \quad (43)$$

where the state $|\psi\rangle = e^{-i\frac{\pi}{2}J_1} |\text{Lagu}\rangle$ is the correlated probe state after the input state $|\text{Lagu}\rangle$ is injected into the first optical BS (BS1) of MZI, and Hermitian operators $\hat{H}_{1,2}$ are defined by

$$\begin{aligned} \hat{H}_1 &= \sum_l \frac{d\hat{\Pi}_l^\dagger(\varphi)}{d\varphi} \frac{d\hat{\Pi}_l(\varphi)}{d\varphi}, \\ \hat{H}_2 &= i \sum_l \frac{d\hat{\Pi}_l^\dagger(\varphi)}{d\varphi} \hat{\Pi}_l(\varphi), \end{aligned} \quad (44)$$

where $\hat{\Pi}_l(\varphi)$ are Kraus operators, i.e.,

$$\hat{\Pi}_l(\varphi) = \sqrt{\frac{(1-\eta)^l}{l!}} e^{-i\varphi\left(\frac{a^\dagger a - b^\dagger b}{2} + \frac{\gamma l}{2}\right)} \eta^{\frac{b^\dagger b}{2}} b^l. \quad (45)$$

where $\gamma = 0$ and $\gamma = -1$ represent the photon losses before and after the phase shifter, respectively. η is related to the dissipation factor with $\eta = 1$ and $\eta = 0$ being the cases of complete lossless and absorption, respectively.

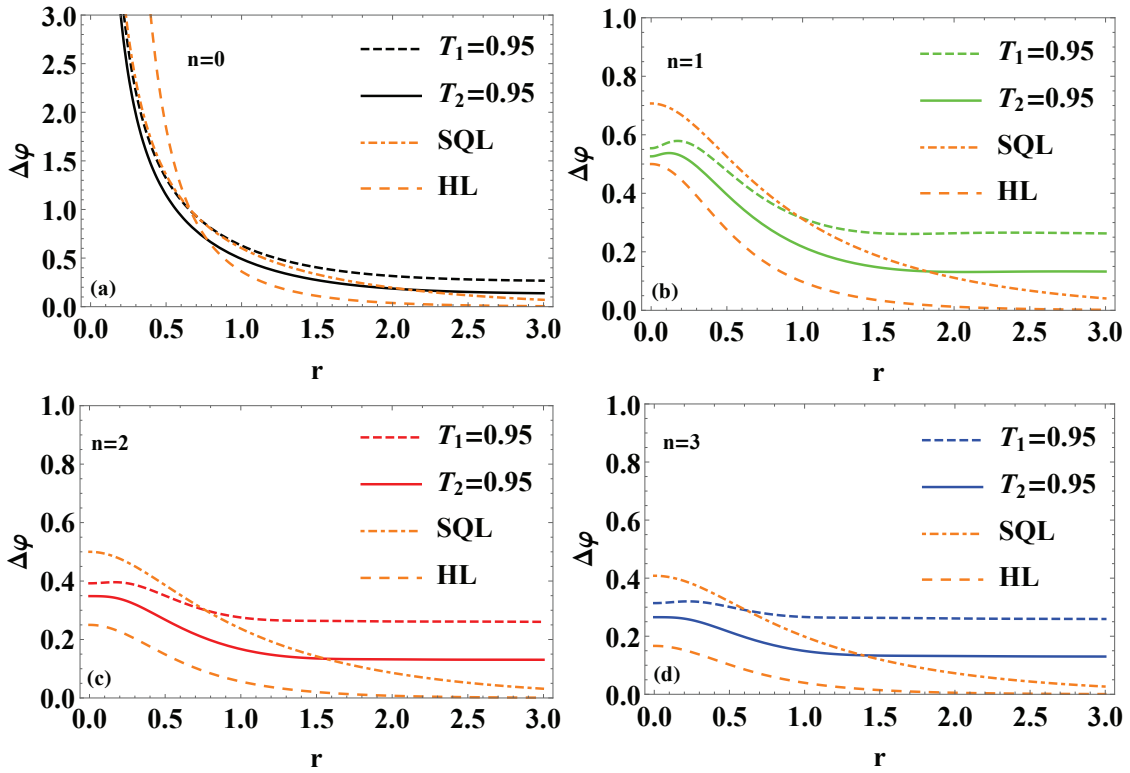


FIG. 8: The phase sensitivity $\Delta\varphi$ as a function of the squeezing parameters r in the case of photon losses comparing with the SQL and the HL (a) for $\varphi = 0.2$, $n = 0$ and T_1 or $T_2 = 0.96$. (b) for $\varphi = 0.15$, $n = 1$ and T_1 or $T_2 = 0.95$. (c) for $\varphi = 0.12$, $n = 2$ and T_1 or $T_2 = 0.95$. (d) for $\varphi = 0.1$, $n = 3$ and T_1 or $T_2 = 0.95$.

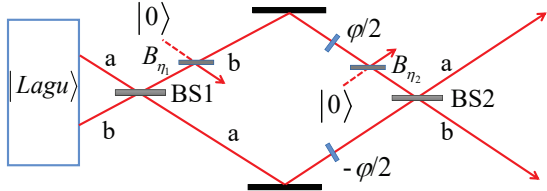


FIG. 9: Schematic diagram of a lossy interferometer. The losses of mode b in the interferometer are modeled by adding the fictitious beam splitters before and after the phase shift.

By combining Eqs. (43)-(45) for further calculation, we can get

$$C_Q = \langle \Delta^2 \hat{n}_a \rangle + (\eta + \gamma\eta - \gamma)^2 \langle \Delta^2 \hat{n}_b \rangle - 2(\eta + \gamma\eta - \gamma) \text{Cov}[\hat{n}_a, \hat{n}_b] + (1 + \gamma)^2 \eta(1 - \eta) \langle \hat{n}_b \rangle, \quad (46)$$

where $\hat{n}_a = a^\dagger a$, $\hat{n}_b = b^\dagger b$, $\langle \Delta^2 \hat{n}_i \rangle = \langle \hat{n}_i^2 \rangle - \langle \hat{n}_i \rangle^2$ ($i = a, b$), and $\text{Cov}[\hat{n}_a, \hat{n}_b] = \langle \hat{n}_a \hat{n}_b \rangle - \langle \hat{n}_a \rangle \langle \hat{n}_b \rangle$ ($\langle \cdot \rangle = \langle \psi | \cdot | \psi \rangle$). Minimizing over the parameter γ in Eq. (46) will lead to the minimum value of C_Q in the presence of photon losses, where the optimal value of γ can be obtained

$$\gamma_{opt} = \frac{\eta \langle \Delta^2 \hat{n}_b \rangle - \text{Cov}[\hat{n}_a, \hat{n}_b] - \eta \langle \hat{n}_b \rangle}{(1 - \eta) \langle \Delta^2 \hat{n}_b \rangle + \eta \langle \hat{n}_b \rangle}. \quad (47)$$

Thus substituting Eq. (47) into Eq. (46), the minimum value of C_Q can be ready to obtain.

Using Eqs. (1) and (3) and the transform relations

$$\begin{aligned} e^{i\frac{\pi}{2}J_1} a e^{-i\frac{\pi}{2}J_1} &= \frac{\sqrt{2}}{2} (a - ib), \\ e^{i\frac{\pi}{2}J_1} b e^{-i\frac{\pi}{2}J_1} &= \frac{\sqrt{2}}{2} (b - ia), \end{aligned} \quad (48)$$

one can obtain

$$\begin{aligned} \langle \hat{n}_a \rangle &= \langle \hat{n}_b \rangle = n \cosh^2 r + (n + 1) \sinh^2 r, \\ \langle \hat{n}_a^2 \rangle &= \langle \hat{n}_b^2 \rangle = (3n^2 + n) \frac{\cosh^4 r}{2} \\ &\quad + (3n^2 + 5n + 2) \frac{\sinh^4 r}{2} \\ &\quad + (3n^2 + 3n + 1) \frac{\sinh^2(2r)}{2}, \end{aligned} \quad (49)$$

and

$$\begin{aligned} \langle \hat{n}_a \hat{n}_b \rangle &= (n^2 - n) \frac{\cosh^4 r}{2} \\ &+ (n^2 + 3n + 2) \frac{\sinh^4 r}{2} \\ &+ (n^2 + n) \frac{\sinh^2(2r)}{2}. \end{aligned} \quad (50)$$

By combining Eq. (46) with Eq. (47) and further using Eq. (49) and Eq. (50), we can get the value of γ_{opt} and the minimum value of C_Q , i.e. the QFI F_Q for the phase shift in the presence of photon losses in MZI, not shown here for simplicity. In particular, for the case of the transmissivity $\eta = 1$ corresponding to the ideal case, the expression for F_Q just reduces to Eq. (11), as expected.

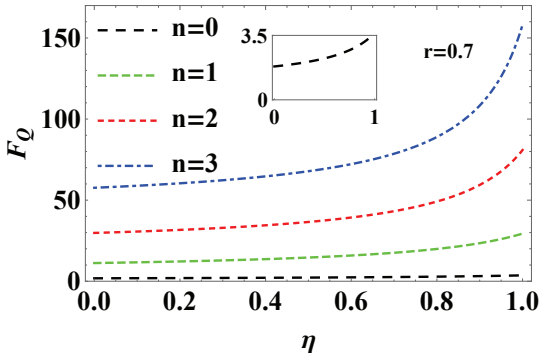


FIG. 10: The quantum Fisher information F_Q as a function of the transmissivity η , for the photon number $n = 0, 1, 2, 3$ and the squeezing parameter $r = 0.7$.

Based on these formula above, we can clearly discuss the relation between QFI and related parameters. In Fig. 10, we present the QFI F_Q as a function of the transmissivity η for different photon number $n = 0, 1, 2, 3$ under given the squeezing parameter ($r = 0.7$). From Fig. 10, it is clearly seen that the F_Q increases with the increase of η or n . This indicates that although photon losses can reduce the QFI, it can be significantly improved by increasing the excited photon number. In addition, with the increasing of η , the increasing of n has more clear improvement on the QFI.

Fig. 11 shows the QFI F_Q and the QCRB as a function of the squeezing parameter r for the different transmissivity $\eta = 1, 0.8$ and excited photon number $n = 0, 1, 2, 3$. It is shown that the F_Q can be increased by increasing the excited photon number n or the squeezing parameter r . In particular, the difference of F_Q between ideal and photon-loss cases increase as n or r , which becomes more clear in the small squeezing region. This implies that, in a realistic case, the F_Q with a higher excited photon-number is more susceptible to the environment, especially in small squeezing region. In addition, the case becomes less obvious in large squeezing region. This case is true for the QCRB where $\Delta\varphi_{QCRB} = 1/\sqrt{F_Q}$, see Fig. 11(b).

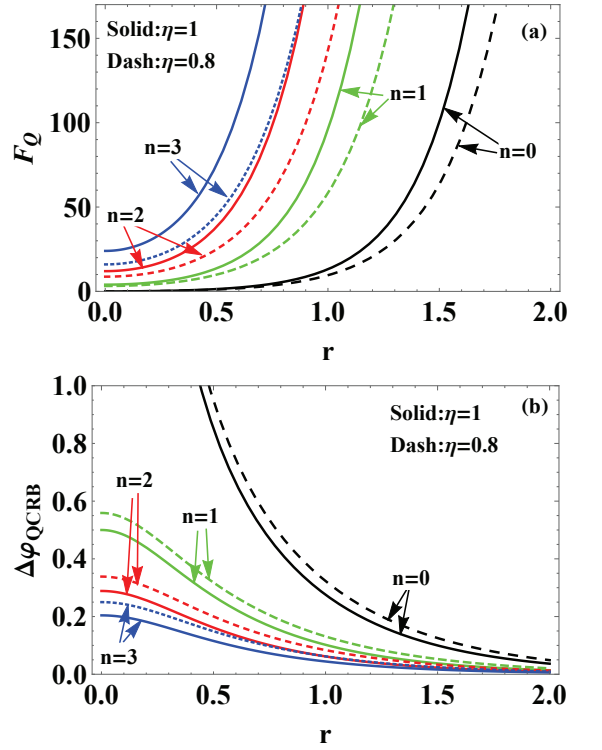


FIG. 11: For the photon number $n = 0, 1, 2, 3$, the transmissivity $\eta = 1$ and $\eta = 0.8$, (a) the quantum Fisher information F_Q as a function of the squeezing parameter r , (b) $\Delta\varphi_{QCRB}$ as a function of r .

In order to further clearly see the relation between the QCRB and the SQL, the HL, we plot the QCRB $\Delta\varphi_{QCRB}$ as a function of the squeezing parameter r for different excited photon number $n = 0, 1, 2, 3$ and both ideal and realistic cases in Fig. 12. Here the SQL and the HL are also plotted for comparison. From Fig. 12, it is clear that (i) for the case of $n = 0$ corresponding to the TMSV, the QCRB can break the SQL and the HL. In fact, considering the TMSVs as inputs of the ideal MZI, it is found that $\Delta\varphi_{QCRB} = \frac{1}{\sqrt{N^2+2N}}$, which exceeds the HL defined as $\frac{1}{N}$ [27]. (ii) for the cases of $n = 1, 2, 3$, the QCRB is between the SQL and the HL. In particular, for the ideal case of $\eta = 1$, the QCRB with $n = 1$ basically coincides with the HL. (iii) the QCRB can almost saturate the HL as the increasing of r . Although the QCRB breaks the HL at $n = 0$, the QCRB can still be improved with increasing n . In addition, the difference between ideal and realistic cases becomes smaller with increasing r . These results imply that although the QCRB can break the HL for the TMSV, the QCRB can be further improved by introducing excited photon number.

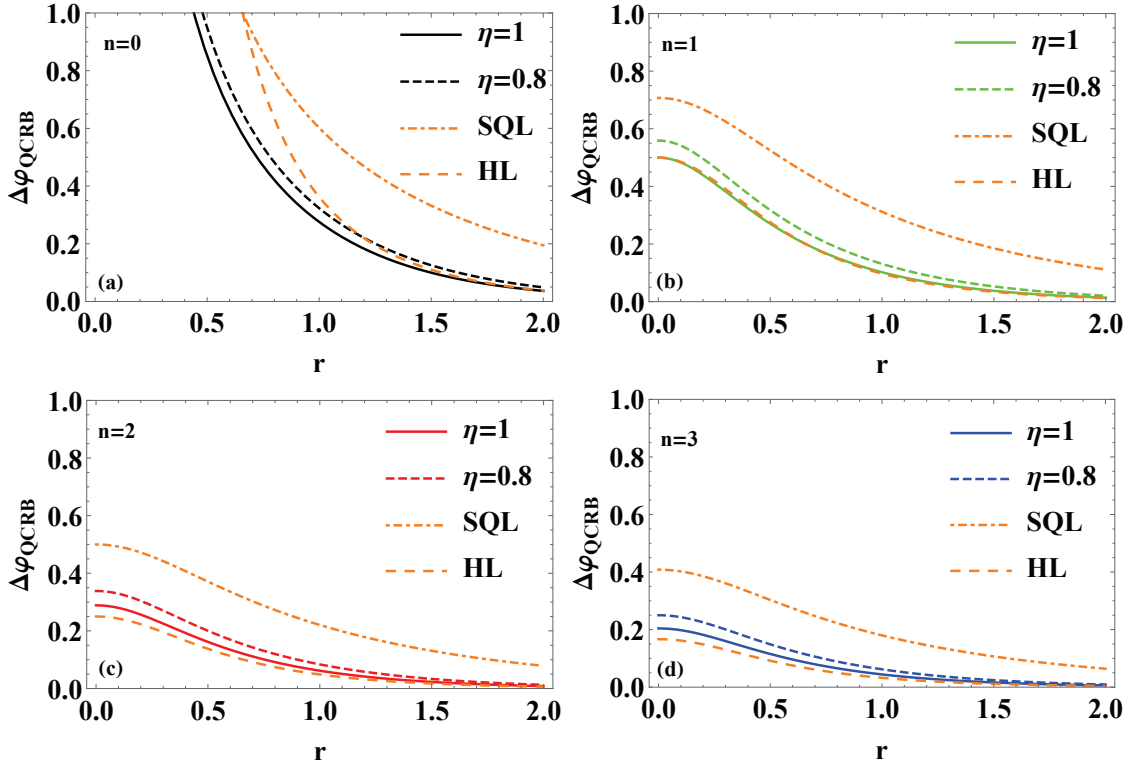


FIG. 12: $\Delta\varphi_{QCRB}$ as a function of the squeezing parameter r comparing with the SQL and the HL (a) for $n = 0$, $\eta = 1, 0.8$, (b) for $n = 1$, $\eta = 1, 0.8$, (c) for $n = 2$, $\eta = 1, 0.8$, (d) for $n = 3$, $\eta = 1, 0.8$.

V. CONCLUSION

In summary, we introduced a kind of non-Gaussian state, i.e., Laguerre polynomial excited squeezed state as input of the traditional MZI. Then we first investigated the phase sensitivity with parity detection and the QFI in ideal case. In particular, we derived an equivalent operator by using the Weyl ordering invariance under similarity transformations, whose normal ordering form is given. It is convenient to calculate the average of parity operator using the equivalent operator for any input state of the traditional MZI. This method is also effect when considering the realistic case.

We further examined the effects of photon losses on the phase sensitivity, including internal and external losses. It is found that the external loss presents a bigger influence than the internal one. Moreover, the phase sensitivity can be improved with the increase of the excited photon number n for any squeezing parameter r . Specially speaking, the optimal phase sensitivity is at the point with $\varphi = 0$, and becomes better as n increases for the ideal case. For the realistic case, however, the optimal point of the phase sensitivity will deviate from $\varphi = 0$, and the $\Delta\varphi$ value corresponding to optimal point decreases with the increase of n . It is interesting that even in the realistic case, the phase sensitivity still surpass that

by the TMSV in the ideal case, but the improved region of φ becomes smaller with the increase of n . When fixing the total input photon number, the phase sensitivity can also be enhanced by increasing n in the realistic case, although this case is not true in the ideal case.

In addition, we investigated the effects of photon losses on the QFI. It is shown that although the QFI will reduce due to the photon losses, it can still increase as the squeezing parameter r or the photon number n . But the F_Q with a higher excited photon-number is more susceptible to the environment, which becomes more clear in the small squeezing region. The QCRB $\Delta\varphi_{QCRB}$ can break the SQL and even beat the HL, which can be further improved by introducing excited photon number. These results can be effectively applied to improve the accuracy of phase measurement in the realistic case.

Acknowledgments

This work is supported by the National Natural Science Foundation of China (Grants No. 11964013 and No. 11664017) and the Training Program for Academic and Technical Leaders of Major Disciplines in Jiangxi Province (No. 20204BCJL22053).

-
- [1] J. G. Rarity, P. R. Tapster, E. Jakeman, T. Larchuk, R. A. Campos, M. C. Teich, and B. E. A. Saleh, Two-photon interference in a Mach-Zehnder interferometer, *Phys. Rev. Lett.* **65**, 1348 (1990).
- [2] M. O. Scully and M. S. Zubairy, *Quantum Optics* (Cambridge University Press, Cambridge, 1997).
- [3] P. Luca and S. Augusto, Mach-Zehnder Interferometry at the Heisenberg Limit with Coherent and Squeezed-Vacuum Light, *Phys. Rev. Lett.* **100**, 073601 (2008).
- [4] X. Yu, X. Zhao, L. Y. Shen, Y. Y. Shao, J. Liu, and X. G. Wang, Maximal quantum Fisher information for phase estimation without initial parity, *Opt. Express* **26**, 16292 (2018).
- [5] V. Giovannetti, S. Lloyd, and L. Maccone, Advances in quantum metrology, *Nat. Photon.* **5**, 222 (2011).
- [6] C. W. Helstrom, *Quantum detection and estimation theory* (Academic, New York, 1976).
- [7] C. M. Caves, Quantum-mechanical noise in an interferometer, *Phys. Rev. D* **23**, 1693 (1981).
- [8] A. N. Boto, P. Kok, D. S. Abrams, S. L. Braunstein, C. P. Williams, and J. P. Dowling, Quantum interferometric optical lithography: exploiting entanglement to beat the diffraction limit, *Phys. Rev. Lett.* **85**, 2733 (2000).
- [9] R. A. Campos, Christopher C. Gerry, and A. Benmoussa, Optical interferometry at the Heisenberg limit with twin Fock states and parity measurements, *Phys. Rev. A* **68**, 023810 (2003).
- [10] P. M. Anisimov, G. M. Raterman, A. Chiruvelli, W. N. Plick, S. D. Huver, H. Lee, and J. P. Dowling, Quantum Metrology with Two-Mode Squeezed Vacuum: Parity Detection Beats the Heisenberg Limit, *Phys. Rev. Lett.* **104**, 103602 (2010).
- [11] H. Lee, P. Kok, and J. P. Dowling, A quantum Rosetta stone for interferometry, *J. Mod. Opt.* **49**, 2325 (2002).
- [12] T. Nagata, R. Okamoto, J. L. O'Brien, K. Sasaki, and S. Takeuchi, Beating the Standard Quantum Limit with Four-Entangled Photons, *Science*, **316**, 726 (2007).
- [13] J. P. Dowling, Quantum optical metrology – the lowdown on high-NOON states, *Contemp. Phys.* **49**, 125 (2008).
- [14] G. Y. Xiang, B. L. Higgins, D. W. Berry, H. M. Wiseman, and G. J. Pryde, Entanglement-enhanced measurement of a completely unknown optical phase, *Nat. Photon.* **5**, 43 (2011).
- [15] H. Cable and G. A. Durkin, Parameter Estimation with Entangled Photons Produced by Parametric Down-Conversion, *Phys. Rev. Lett.* **105**, 013603 (2010).
- [16] T. Eberle, V. Hädchen, and R. Schnabel, Stable control of 10 dB two-mode squeezed vacuum states of light, *Opt. Express*, **21**, 11546 (2013).
- [17] M. A. Rubin and S. Kaushik, Loss-induced limits to phase measurement precision with maximally entangled states, *Phys. Rev. A* **75**, 053805 (2007).
- [18] K. Jiang, C. J. Bragnac, Y. Weng, M. B. Kim, H. Lee, and J. P. Dowling, Strategies for choosing path-entangled number states for optimal robust quantum-optical metrology in the presence of loss, *Phys. Rev. A* **86**, 013826 (2012).
- [19] M. W. Mitchell, J. S. Lundeen, and A. M. Steinberg, Super-resolving phase measurements with a multiphoton entangled state, *Nature*, **429**, 161 (2004).
- [20] I. Afek, O. Ambar, and Y. Silberberg, High-NOON States by Mixing Quantum and Classical Light, *Science*, **328**, 879 (2010).
- [21] J. C. F. Matthews, A. Politi, D. Bonneau, and J. L. O'Brien, Heralding Two-Photon and Four-Photon Path Entanglement on a Chip, *Phys. Rev. Lett.* **107**, 163602 (2011).
- [22] C. C. Gerry and J. Mimih, Heisenberg-limited interferometry with pair coherent states and parity measurements, *Phys. Rev. A* **82**, 013831 (2010).
- [23] L. Y. Hu, M. Al-amri, Z. Y. Liao, and M. S. Zubairy, Continuous-variable quantum key distribution with non-Gaussian operations, *Phys. Rev. A* **102**, 012608 (2020).
- [24] P. Marian and T. A. Marian, Continuous-variable teleportation in the characteristic-function description, *Phys. Rev. A* **74**, 042306 (2006).
- [25] L. L. Guo, Y. F. Yu, and Z. M. Zhang, Improving the phase sensitivity of an SU(1,1) interferometer with photon-added squeezed vacuum light, *Opt. Express*, **26**, 029099 (2018).
- [26] R. Carranza and C. C. Gerry, Photon-subtracted two-mode squeezed vacuum states and applications to quantum optical interferometry, *J. Opt. Soc. Am. B* **29**, 2581 (2012).
- [27] Y. Ouyang, S. Wang, and L. J. Zhang, Quantum optical interferometry via the photon-added two-mode squeezed vacuum states, *J. Opt. Soc. Am. B* **33**, 1373 (2016).
- [28] R. Birrittella, J. Mimih, and C. C. Gerry, Multiphoton quantum interference at a beam splitter and the approach to Heisenberg-limited interferometry, *Phys. Rev. A* **86**, 063828 (2012).
- [29] D. Braun, P. Jian, O. Pinel, and N. Treps, Precision measurements with photon-subtracted or photon-added Gaussian states, *Phys. Rev. A* **90**, 013821 (2014).
- [30] S. K. Chang, C. P. Wei, H. Zhang, Y. Xia, W. Ye, and L. Y. Hu, Enhanced phase sensitivity with a nonconventional interferometer and nonlinear phase shifter, *Phys. Lett. A* **384**, 126755 (2020).
- [31] S. K. Chang, W. Ye, H. Zhang, L. Y. Hu, J. H. Huang, and S. Q. Liu, Improvement of phase sensitivity in an SU(1,1) interferometer via a phase shift induced by a Kerr medium, *Phys. Rev. A* **105**, 033704 (2022).
- [32] Q. K. Gong, X. L. Hu, D. Li, C. H. Yuan, Z. Y. Ou, and W. P. Zhang, Intramode-correlation-enhanced phase sensitivities in an SU(1,1) interferometer, *Phys. Rev. A* **96**, 033809 (2017).
- [33] R. Birrittella and C. C. Gerry, Quantum optical interferometry via the mixing of coherent and photon-subtracted squeezed vacuum states of light, *J. Opt. Soc. Am. B* **31**, 586 (2014).
- [34] S. Wang, X. X. Xu, Y. J. Xu, and L. J. Zhang, Quantum interferometry via a coherent state mixed with a photon-added squeezed vacuum state, *Opt. Commun.* **444**, 102 (2019).
- [35] H. Zhang, W. Ye, C. P. Wei, Y. Xia, S. K. Chang, Z. Y. Liao, and L. Y. Hu, Improved phase sensitivity in quantum optical interferometer based on multi-photon catalytic two-mode squeezed vacuum states, *Phys. Rev. A* **103**, 013705 (2021).
- [36] H. Zhang, W. Ye, C. P. Wei, C. J. Liu, Z. Y. Liao, and L. Y. Hu, Improving phase estimation using the number-conserving operations, *Phys. Rev. A* **103**, 052602 (2021).
- [37] W. Ye, W. D. Zhou, H. L. Zhang, C. J. Liu, J. H. Huang, and L. Y. Hu, Laguerre polynomial excited coherent state: generation and nonclassical properties, *Laser Phys. Lett.*

- 14, 115021 (2017).
- [38] L. Y. Hu and Z. M. Zhang, Nonclassicality and decoherence of photon-added squeezed thermal state in thermal environment, *J. Opt. Soc. Am. B* **29**, 529 (2012).
- [39] L. Y. Hu and H. Y. Fan, Two-Variable Hermite Polynomial Excitation of Two-Mode Squeezed Vacuum State as Squeezed Two-Mode Number State, *Commun Theor. Phys.* **50**, 965 (2008).
- [40] G. Y. Xiang, H. F. Hofmann, and G. J. Pryde, Optimal multi-photon phase sensing with a single interference fringe, *Sci. Rep.* **3**, 2684 (2013).
- [41] B. Yurke, S. L. McCall, and J. R. Klauder, SU(2) and SU(1,1) interferometers, *Phys. Rev. A* **33**, 4033 (1986).
- [42] H. Y. Fan and L. Y. Hu, Two quantum-mechanical photon-count formulas, *Opt. Lett.* **33**, 443 (2008).
- [43] H. Y. Fan and L. Y. Hu, New n-mode squeezing operator and squeezed states with standard squeezing, *EPL*, **85**, 60001 (2009).
- [44] H. Y. Fan, Newton–Leibniz integration for ket-bra operators in quantum mechanics (V)—Deriving normally ordered bivariate-normal-distribution form of density operators and developing their phase space formalism, *Ann. Phys. (NY)* **323**, 1502 (2008).
- [45] H. Weyl, Quantenmechanik und Gruppentheorie, *Z. Phys.* **46**, 1 (1927).
- [46] E. P. Wigner, On the Quantum Correction for Thermodynamic Equilibrium, *Phys. Rev.* **40**, 749 (1932).
- [47] H. Y. Fan and H. R. Zaidi, Application of IWOP technique to the generalized Weyl correspondence, *Phys. Lett. A* **124**, 303 (1987).
- [48] H. Y. Fan, H. R. Zaidi, and J. R. Klauder, New approach for calculating the normally ordered form of squeeze operators, *Phys. Rev. D* **35**, 1831 (1987).
- [49] R. R. Puri, *Mathematical methods of quantum optics* (Springer-Verlag, Berlin, 2001), Appendix A.
- [50] B. M. Escher, R. L. de Matos Filho, and L. Davidovich, General framework for estimating the ultimate precision limit in noisy quantum-enhanced metrology, *Nature* **7**, 406 (2011).